An *ex vivo* investigation into the transurothelial permeability and bladder wall distribution of the non-steroidal anti-inflammatory ketorolac

Nicholas A. Williams [a], *Jenna L. Bowen* [a], *Ghaith Al-Jayyoussi* [a], *Mark Gumbleton* [a], *Chris J. Allender* [a*], *Jamie Li* [b], *Tim Harrah* [b], *Aditya Raja* [c], *Hrishi B. Joshi* [c].

[a]School of Pharmacy and Pharmaceutical Sciences, Cardiff University, Redwood Building, King Edward VII Ave., Cardiff, UK

[b]Urology & Women's Health, Boston Scientific Corporation, 100 Boston Scientific Way, Marlborough, MA, 01752, USA.

[c]Department of Urology, University Hospital of Wales, Cardiff, UK

[*]Chris J. Allender, PhD
Room 0.45, School of Pharmacy and Pharmaceutical Sciences, Cardiff University, Redwood Building, King Edward VII Ave, Cardiff, UK, CF10 3NB
Tel. +44 (0)29 208 75824
Fax. +44 (0)29 208 74149
Email. allendercj@cf.ac.uk

ABSTRACT

Transurothelial drug delivery continues to be an attractive treatment option for a range of urological conditions, however dosing regimens remain largely empirical. Recently, intravesical delivery of the non-steroidal anti-inflammatory ketorolac has been shown to significantly reduce ureteral stent-related pain. While this latest development provides an opportunity for advancing in the management of stent-related pain, its translation into effective patient management will undoubtedly benefit from an understanding of the rate and extent of delivery of ketorolac into the bladder wall. Using an *ex vivo* porcine model, we evaluate the urothelial permeability and bladder wall distribution of ketorolac. The subsequent application of a pharmacokinetic (PK) model enables prediction of concentrations achieved *in vivo*.

Ketorolac was applied to the urothelium and a transurothelial permeability coefficient (K_p) calculated. Relative drug distribution into the bladder wall after 90 minutes was determined. Ketorolac was able to permeate the urothelium (K_p = 2.63 x 10^{-6} cm s^{-1}) and after 90 minutes average concentrations of 400, 141 and 21 µg g^{-1} were achieved in the urothelium, lamina propria and detrusor respectively. An average concentration of 87 µg g^{-1} was achieved across the whole bladder wall. PK simulations (STELLA®) were then carried out, using *ex vivo* values for K_p and muscle/saline partition coefficient (providing an estimation of vascular clearance), to predict 90 minutes *in vivo* ketorolac tissue concentrations. When dilution of the drug solution with urine and vascular clearance were taken into account, a reduced ketorolac concentration of 37 µg g^{-1} across the whole bladder wall was predicted.

These studies reveal crucial information about the urothelium's permeability to agents such as ketorolac and the concentrations achievable in the bladder wall. It would appear that levels of

ketorolac delivered to the bladder wall intravesically would be sufficient to provide an anti-inflammatory effect. The combination of such *ex vivo* data and PK modelling provides an insight into the likelihood of achieving clinically relevant concentrations of drug following intravesical administration.

Key words: Intravesical; Ketorolac; Pharmacokinetics; Urothelium; Stent

1. Introduction

Intravesical drug delivery (IDD), the most common form of transurothelial drug delivery, takes advantage of the bladder's unique anatomy to allow the prolonged exposure of high concentrations of drug to the bladder's luminal surface, whilst minimising systemic absorption. IDD therefore overcomes the shortcomings of systemic therapy, which is often ineffective due to poor bladder bioavailability and unwanted adverse effects [1,2].

However, the effectiveness of IDD is limited by several intrinsic properties of the bladder. A specialised, highly impermeable epithelial layer, known as the urothelium, lines the luminal surface. The urothelium is an exceptional barrier with reported transepithelial resistances ranging from 10,000 to 75,000 Ω cm^2 [3]; these represent some of the highest values of all epithelia measured to date [4]. The urothelium is the primary barrier to the movement of molecules from the urine into the blood and will limit the extent to which drugs can permeate into the bladder wall [1]. Additionally urine flows into the bladder at a constant rate (~1 ml min^{-1}) [5] diluting the concentration of instilled drug and the need to regularly void the bladder means any drug load will subsequently be lost, reducing exposure time to the bladder wall. Whilst IDD has historically been used as a method for delivering drugs locally to the lower urinary tract, it is inevitable that future developments will seek to improve both controllability and sustainability of therapeutic strategies by incorporating drugs into devices such as ureteral stents [6,7].

Despite having been used for a number of decades, intravesical dosing regimens remain largely empirical. This subject has received some attention with investigations into the bladder wall permeation of common intravesical solutions [8–10], as well as the effect of permeation enhancers such as chitosan and dimethyl sulfoxide [11–13]. Recently it has been shown that enhanced bladder

wall uptake can be achieved using nanoparticle delivery systems for superficial bladder cancer [14–18].

Despite this, many questions remain unanswered about the ability of different drugs to permeate across the urothelium and ultimately the viability of delivering drugs in this manner. *In vivo* data from IDD studies is limited, due to the difficulty in obtaining bladder tissue concentrations in human and animal subjects, and therefore dosing regimens are typically based on perceived clinical benefits. Although qualitative end points are clinically useful, quantitative data on urothelial permeability and bladder tissue distribution is far more important when predicting the usefulness of new local drug delivery approaches. Research of this kind has clear clinical translation and is key if we are to maximise the potential of delivering drugs locally to the urinary tract.

The primary aim of the current study was to improve our knowledge of IDD by probing the permeability of the bladder wall in an *ex vivo* setting. To this end we have investigated ketorolac, a non-steroidal anti-inflammatory drug (NSAID) commonly used in urological practice in the US, as an exemplar. We describe an *ex vivo* approach for estimating local tissue drug concentrations achievable after IDD, which can be used not only to predict the usefulness of prospective therapies but also to optimise existing dosing regimens.

2. Experimental section

2.1. Bladder preparation

Porcine bladders, from pigs weighing 70-90 kg, were obtained fresh from a local abattoir within five minutes of excision and transported in ice-cold oxygenated Krebs buffer back to the laboratory. Bladders were filled and drained with 37 °C saline to remove any residual urine. Using a scalpel, excess perivesical fat was trimmed away and a single straight-line incision made along the length of the bladder exposing the right and left lateral sides. The bladder was cut into 2 cm^2 sections from the lateral sides and dome area and loaded into glass Franz-type diffusion cells (Figure 1) (Permegear Inc, Hellertown, PA, USA) with the urothelium facing upwards. Care was taken to avoid contact with the urothelial surface and a metal clamp was used to secure the tissue between the donor and receiver chambers of the in the Franz-type cells. The receptor compartment was filled with oxygenated Krebs buffer and equilibrated at 37 °C for 30 min with a micro stirrer bar providing continuous stirring. A solution of the drug was pipetted into the donor chamber which was covered with a glass disc to prevent evaporative loss. The sampling arm was capped and the Franz-type cells placed in to a thermostatically controlled water bath, maintained at 37 °C, on top of a submersible magnetic stirrer plate.

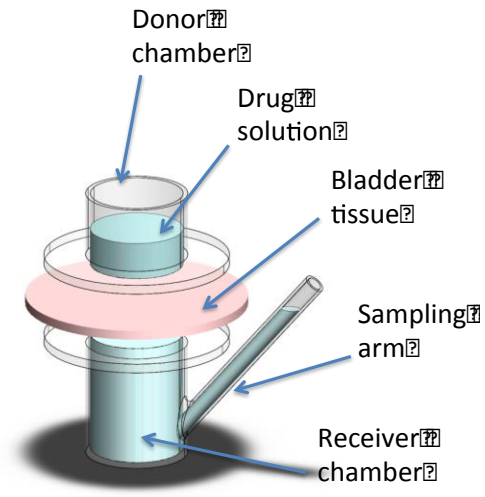

Fig 1. Schematic of a Franz-type diffusion cell loaded with porcine bladder tissue

2.2. Confirmation of tissue viability

2.2.1. Investigating paracellular marker permeability

The viability of the bladder tissue over 5 h was evaluated in an assay investigating the co-permeation of propranolol hydrochloride (≥ 99%, Acros Organics, Geel, Belgium) and sodium fluorescein (≥ 95%, Sigma-Aldrich Ltd, Dorset, England) across the urothelium and lamina propria. A 500 µl aliquot of a saline solution of 1 mM propranolol hydrochloride and 0.1 mM sodium fluorescein was added to the donor chamber of the Franz-type cell. At fixed time points (0.5, 1.5, 3.5 and 5 h), the contents of the receptor and donor chambers were collected and the tissue sample removed.

Prior to removal with a cork borer, the area of tissue in contact with the drug was subjected to three saline rinses (1 ml each rinse) to remove any adsorbed drug and the urothelium and lamina propria carefully separated from the underlying detrusor muscle by cutting along the natural

plane of division with a scalpel. Tissue sections were weighed and drug recovered by repeated extraction in methanol.

Propranolol hydrochloride was analysed using HPLC (Kromasil C18 column, 5 μm, 250 mm x 4.6 mm i.d column, Supelco Inc). The mobile phase consisted of 70 % acetonitrile : 30 % sodium dodecyl sulfate (10 mM), disodium hydrogen phosphate (10 mM) adjusted to pH 2.3 with phosphoric acid. UV detection was set at 290 nm. The injection volume was 20 μl and a flow rate of 1 ml min^{-1} was used.

Sodium fluorescein was analysed using a FLUOstar OPTIMA platereader (BMG Labtech GmbH, Ortenburg, Germany) set at an excitation wavelength of 485 nm and emission wavelength of 520 nm.

To ensure accurate separation of the bladder mucosa from the detrusor muscle, histology was performed. The urothelium and lamina propria were removed from one half of a bladder section, with the other half remaining as full thickness bladder tissue. Tissue samples were fixed to cork mounts with optimal cutting temperature medium (OCT) (Tissue-Tek™, CRYO-OCT Compound, Fisher Scientific UK Ltd, Leicestershire, England) and snap frozen in a dry ice-hexane bath. Samples were sectioned at 10 μm using a cryostat (Leica CM3050 S, Leica Microsystems, Buckinghamshire, England). Sections were then stained with haematoxylin-eosin (H&E) for examination by light microscopy.

2.2.2. Transepithelial electrical resistance

The integrity of urothelial, paracellular tight junctions was investigated by measuring any change in the transepithelial electrical resistance (TEER) across the bladder mucosa over time. The

urothelium and lamina propria was carefully removed and a 1 x 1 cm^2 section mounted into an Ussing chamber (NaviCyte vertical multichannel Ussing chambers, Warner Instruments, Hamden, CT, USA). The mucosal chamber was filled with 4 mls of either normal saline or ketorolac 1.1 mg ml^{-1} in saline, whilst the serosal chamber was filled with 4 mls of oxygenated Krebs buffer. The Ussing chambers were maintained at 37 °C and after a 10 minute equilibration period, TEER across the mucosa measured at 15 minute intervals. The TEER value at time zero was taken to be the baseline reading, from which the percentage change from baseline TEER was calculated. To account for any basal resistance of the setup, Ussing chambers were prepared as above but without any bladder mucosa loaded. TEER values were then subtracted from tissue readings and the net electrical resistance of the mucosa multiplied by the apparent exposed tissue area (0.12 cm^2) of the Ussing chamber to yield the TEER. Percentage change from baseline TEER was compared for the saline and ketorolac groups with statistical analysis performed using GraphPad Prism version 6.0c (GraphPad Software, Inc, La Jolla, CA, USA). TEER was measured using a multi-channel voltage–current clamp (EC-800 single channel, Warner Instruments, Hamden, CT, USA). The Ussing chambers were equipped with two pairs of Ag / AgCl electrodes, for measuring potential difference (V) and for passing current (I). The experiments were performed under open circuit conditions, whereby the current was set to zero and the natural transepithelial potential differende could be observed. Electrical readings were recorded every 15 minutes. Electrical resistance was determined according to Ohm's law (R = V / I).

2.2.3. Scanning electron microscopy

To investigate the possibility of urothelial cell desquamation or morphological changes to urothelial surface, bladder tissue was examined by scanning electron microscopy (SEM). Bladder sections were loaded into Franz-type diffusion cells and 500µl of normal saline, ketorolac 1.1 mg ml^{-1} in saline or protamine sulfate 10 mg ml^{-1} in saline added to the donor chamber. After 90 minutes the contents of the donor chambers were removed, the urothelial surface subjected to three saline rinses (1 ml each rinse) and the tissue sample removed. An additional sample, which was fixed at the abattoir approximately 10 minutes after slaughter, was examined as a control. Sections of tissue (2 x 2 cm^2) were carefully cut without touching the urothelial surface and fixed in a solution of 4% formaldehyde and 0.2% glutaraldehyde in 0.1 M phosphate buffer for 24 hours at room temperature. Following a wash in distilled water (2 x 60 min), tissue samples were dehydrated in isopropyl alcohol solutions of increasing concentrations (50–100%) before undergoing chemical drying in 100% hexamethyldisilazane. Samples were then sputter-coated with gold in an Emscope sputter coater (Emscope, Ashford, Kent, UK) before examination at 5 kV with a scanning electron microscopy (Jeol JSM 840A, Tokyo, Japan). Images were acquired with an ADDA 2 image grabber and processed using Scandium analysis software (Soft Imaging System GmbH, Münster, Germany).

2.3. Evaluation of the delivery of ketorolac to the bladder wall

2.3.1. Permeation of ketorolac across the urothelium

Franz-type cells were assembled as described (2.1) and a 0.5 ml aliquot of a 1.1 mg ml^{-1} ketorolac solution (normal saline) (Ketorolac tris salt, ≥ 99%, Sigma-Aldrich Company Ltd,

Dorset, England) was applied to the donor chamber. At fixed time points (1, 2, 3.5 and 5 h), the contents of the receptor and donor chambers were collected and the tissue sample removed. The tissue was rinsed with saline and the ketorolac extracted as described in 2.2.

Ketorolac was analysed using HPLC (Kromasil C18 column, 5 μm, 25 mm x 4.6 mm i.d column, Supelco Inc). The mobile phase consisted of 60 % 0.02 M phosphate buffer (adjusted to pH 3.5 with phosphoric acid) : 40 % acetonitrile, with UV detection at 315 nm. The injection volume was 20 μl and a flow rate of 1 ml min^{-1} was used.

2.3.2. Distribution of ketorolac into the bladder wall

Franz-type cells were assembled as described (2.1) and a 500 μl aliquot of a 1.1 mg ml^{-1} ketorolac solution (normal saline) was applied to the donor chamber. After 90 min the Franz-type cells were dismantled and the urothelial surface rinsed with saline following collection of the donor and receiver compartments. The area of drug contact was isolated, fixed in OCT and tissue samples sectioned using a cryostat as described (2.2.1). Care was taken to ensure OCT was only present on the serosal side of the tissue. Samples were serially sectioned parallel to the urothelial surface at 50 μm thickness and sections collected in pre-weighed 1.5 ml eppendorf tubes. Tissue sections between 0 and 200 μm (urothelium) were collected individually for analysis, whilst five tissue sections between 200 and 1200 μm (lamina propria) and ten tissue sections between 1200 and 3200 (detrusor muscle) were collected and pooled for analysis. For pooled samples, tissue depths were expressed as the midpoint depth of the sections. Tissue sections were then weighed, extracted in 500 μl methanol for 24 hours and drug quantified using HPLC as described (2.3.1). Average tissue concentrations achieved in the urothelium, lamina

propria, detrusor muscle and whole bladder wall were calculated by dividing the total amount of drug recovered by the total weight of tissue in that layer.

2.4. Determination of the muscle to saline partition coefficient for ketorolac

Detrusor muscle was isolated by removing the urothelium and lamina propria as described (2.2.1) and then turning the tissue over to excise the adventitia and serosa in the same manner. Muscle sections were then weighed, placed in a capped 10 ml glass collecting vial and submerged in 3 ml of 11 μg ml^{-1} ketorolac solution (normal saline). The drug solution was sampled at pre-defined time points (1, 1.5, 2, 4 and 6 h) and at 6 h the muscle section was removed and ketorolac extracted to allow the muscle/saline partition coefficient to be calculated.

2.5. Pharmacokinetic modelling

STELLA® (Structural Thinking Experimental Learning Laboratory with Animation, Isee systems inc, New Hampshire, USA) is a computer program that facilitates the mapping, modelling, simulation and communication of dynamic processes [19]. For this study STELLA® was used to create a PK model of intravesical drug delivery. STELLA® version 10.0.2 software was used to create a basic pharmacokinetic model of IDD allowing the incorporation of vascular drug clearance from the bladder wall and dilution of intravesically instilled drug by urine into our *ex vivo* experiments. This model assumes the lamina propria and detrusor muscle to be one compartment with vascular clearance taking place throughout. This assumption is based on the relative small size of the lamina propria, the presence of intermittent smooth muscle strands in

the lamina propria (muscularis mucosae) [20] and the presence of capillary networks in both layers [21,22].

3. Results

3.1. Confirmation of tissue viability

Sodium fluorescein and propranolol hydrochloride are recognised paracellular and transcellular markers respectively [23,24]. In this study the two compounds have been used to evaluate the integrity of the urothelial barrier over 5 h. The results presented in Figure 2A show the amount permeated through the urothelium and lamina propria for each marker over time calculated by summing the amount of drug extracted from the detrusor muscle and any drug recovered from the receptor compartment. Permeability coefficients (K_p) were calculated to be 5.1×10^{-6} cm s^{-1} and 1.3×10^{-6} cm s^{-1} for propranolol hydrochloride and sodium fluorescein respectively. Figure 2B shows the successful removal of the urothelium and lamina propria (U/LP) leaving the underlying detrusor muscle (M).

Deviation from baseline TEER across the bladder mucosa was investigated after the application of saline and ketorolac to the urothelium (Supplementary data S.1). All mucosa samples used had baseline TEER values greater than 500 $\Omega.cm^2$, indicative of tight epithelia [25]. TEER values decreased marginally with time and after 90 min mucosa exposed to saline and ketorolac exhibited 82 and 85 % of baseline TEER respectively. At the end of the experiment (2.5 h) values were 77 and 78 % of baseline TEER for saline and ketorolac respectively. There was no significant difference in TEER reduction between samples exposed to saline or ketorolac at any timepoint (p = 0.511 for 1.5 h timepoint. Significance calculated using two-tailed, unpaired, student's t-test).

The integrity of the *ex vivo* bladder urothelium was analysed by SEM (Figure 3). Tissue

exposed to saline and ketorolac displayed normal surface morphology as evidenced by the polygonal-shaped umbrella cells (A and B). There is evidence of intact tight junctions between adjacent cells, an example of which has been traced for clarity (green dashed line). The urothelial surface morphology of tissue exposed to saline or ketorolac did not differ from the control sample fixed on-site at the abattoir within 5 minutes of excision (supplementary data S.2). Tissue exposed to protamine sulfate (C) exhibited a different morphology with widened tight junctions,

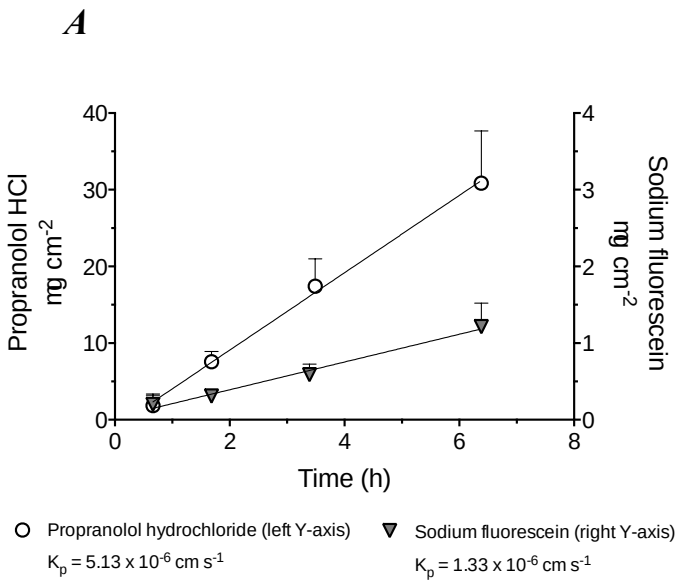

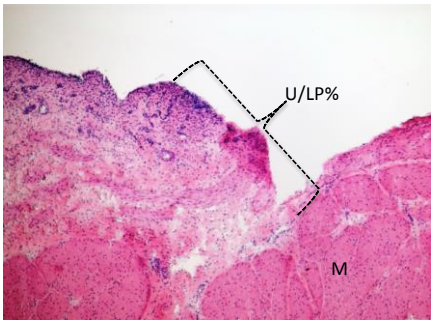

cell lysis (circled red) and apparent shedding of the umbrella cell's apical membrane (red arrow).

Fig 2. (A) Permeation profile of 0.1 mM sodium fluorescein and 1 mM propranolol hydrochloride across porcine urothelium and lamina propria, Permeability coefficients (K_p, cm s^{-1}) were calculated by normalising the flux (J, μg cm^{-2} s^{-1}) to the dosing concentration (A). (n = 4 ± SD, 2 bladders randomised across sampling times). (B) Photomicrograph of a haematoxylin and eosin stained bladder section with the urothelium and lamina propria excised from half the section (400x). U/LP – urothelium and lamina propria, M – detrusor muscle.

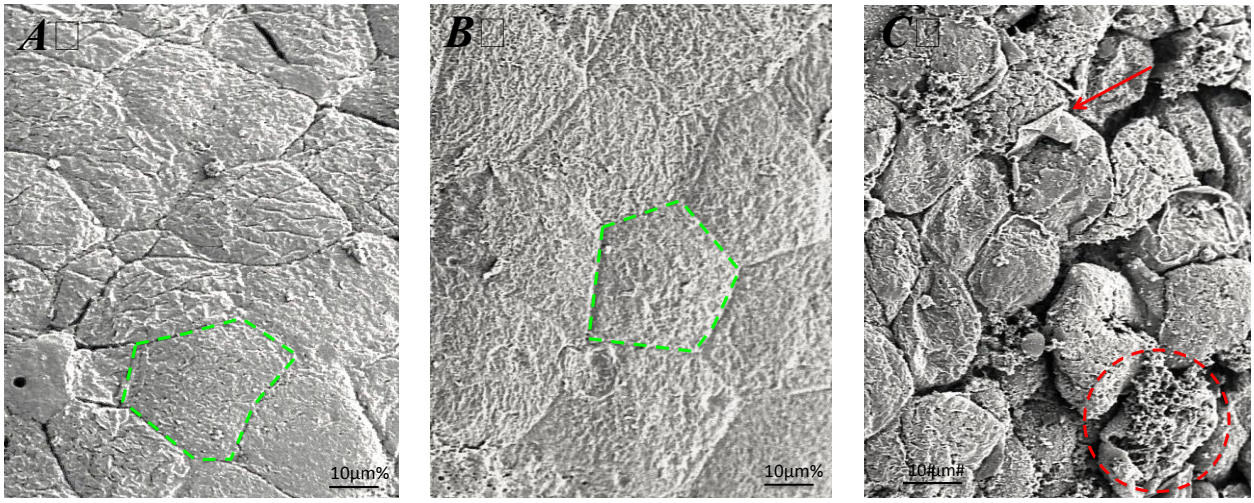

Figure 3. Scanning electron micrographs of *ex vivo* porcine bladder tissue loaded into Franz-type diffusion cells and treated with saline (A), 1.1 mg ml^{-1} ketorolac (B) and 10 mg ml^{-1} protamine sulfate for 90 mins (C). Images show that after exposure to saline and ketorolac the urothelium remains intact (A and B). After exposure to protamine there is a marked loss of barrier integrity (C). (For additional SEM micrographs see supplementary data S.2)

3.2 Permeation of Ketorolac through the bladder wall

In this experiment, unlike in 3.1, there was no separation of the urothelium and lamina propria from the detrusor muscle. This was a case of experimental improvement; studies in our lab showed that after multiple saline washes of the urothelial surface any remaining adsorbed drug was within error of the amounts calculated from tissue extraction. Therefore any drug extracted after the saline rinse is considered to have permeated the urothelium making the separation step unnecessary. Drug that had permeated the urothelium was calculated by summing drug extracted from the tissue and any drug recovered from the receptor compartment. Drug was only present in receiver samples for the 5 hr time point, constituting 0.2% of the applied dose. The profile in Figure 4A shows that after 5 h approximately 60 μg cm^{-2} of ketorolac had permeated into the bladder wall. A K_p value of 2.63 x 10^{-6} cm s^{-1} was calculated for ketorolac across the urothelium. Mass balance studies showed that on average 93% of the applied dose was recovered per sample (Figure 4B).

The distribution of ketorolac into the bladder wall after 90 min is shown in Figure 5. As expected drug concentrations declined with tissue depth with average concentrations of 400, 141 and 21 μg g^{-1} achieved in the urothelium, lamina propria and detrusor muscle respectively. After 90 min the average concentration in the whole bladder wall was calculated to be 87 μg g^{-1}.

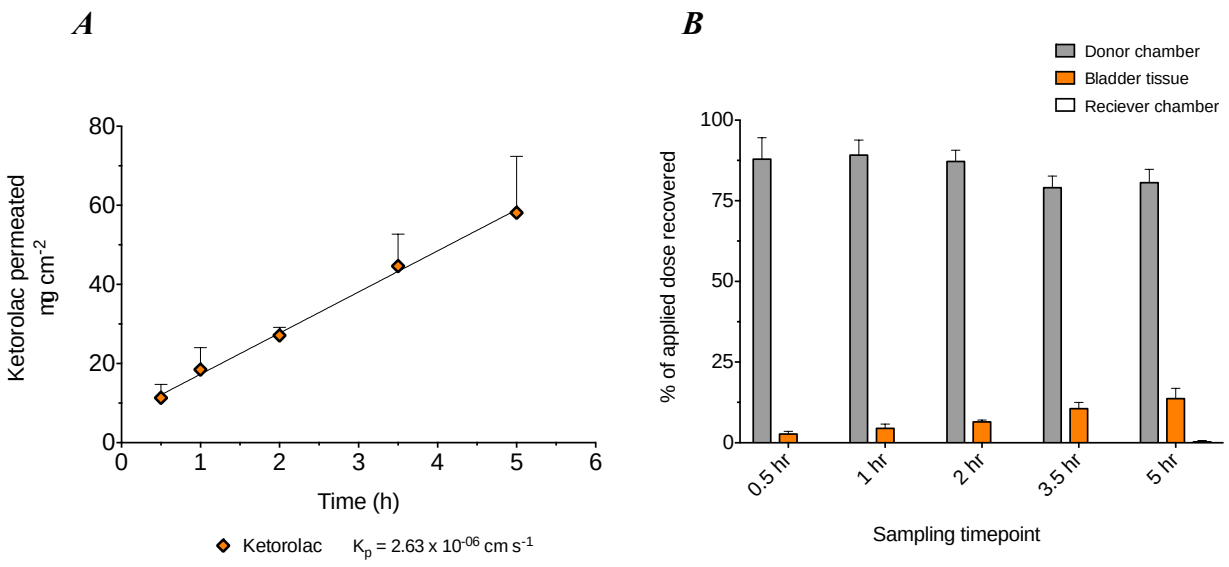

Fig 4. (A) Permeation profile of 1.1 mg ml^{-1} ketorolac across porcine bladder urothelium, Permeability coefficients (K_p, cm s^{-1}) were calculated by normalising the flux (J, μg cm^{-2} s^{-1}) to the dosing concentration. (B) Mass balance analysis of the recovery of ketorolac from the Franz-

type cell setup per sampling timepoint. (n = 4 ± SD, 2 bladders randomised across sampling times).

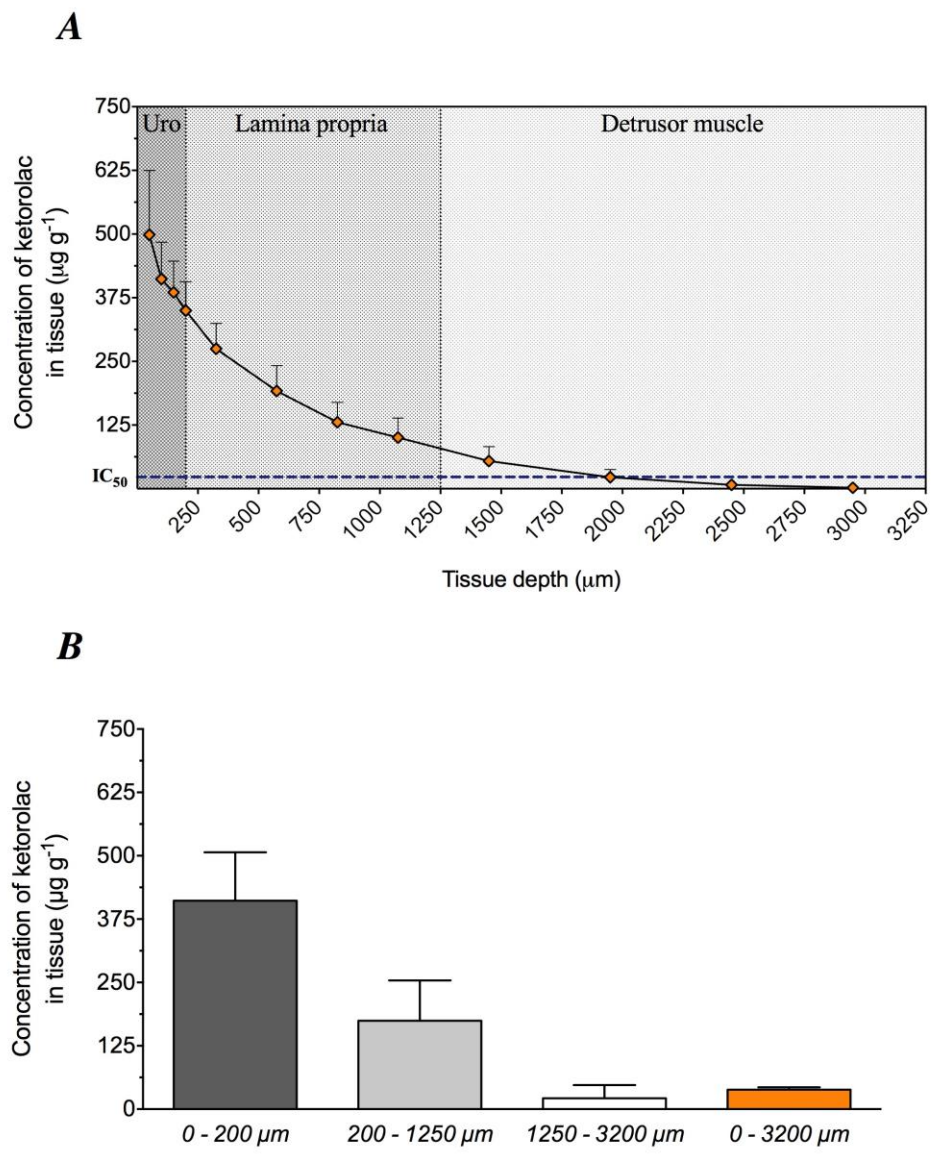

Fig 5. (A) Concentration-depth profile of ketorolac into porcine bladder wall after 90 min. For pooled samples, tissue depths were expressed as the midpoint depth of the sections. IC_{50} represents the top-end value reported at COX-1 and COX-2 for ketorolac[26]. (B) Corresponding average ketorolac concentrations achieved in the urothelium (0-200μm), lamina propria (200-1250μm), detrusor muscle (1250-3200μm) and whole bladder wall (0-3200μm) after 90 min (B). (n = 5 bladders ± SD).

3.3. Determination of the muscle/saline partition coefficient for ketorolac

The concentration of ketorolac solution decreased until equilibrium is established at approximately 2 h (Figure 6A). At equilibrium (2-6 h) the ketorolac concentration was 9.5 µg ml^{-1} and 6.4 µg ml^{-1} in the solution and detrusor muscle respectively (Figure 6B), thus giving a muscle/saline partition coefficient of 0.67.

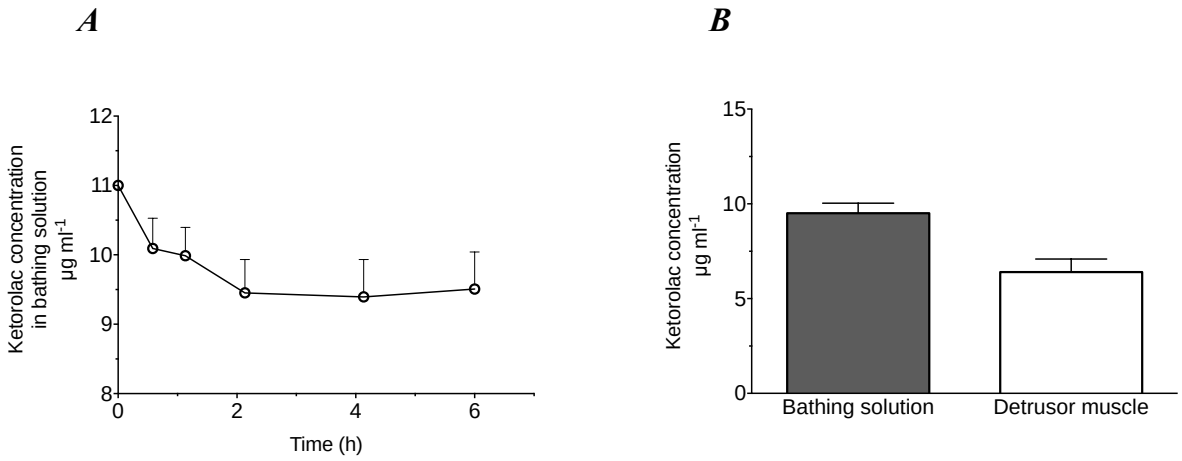

Fig 6. Partition coefficient experiment, showing the concentration of ketorolac in the bathing solution over 6 h (A) and comparison of the concentration of ketorolac in the bathing solution

with that in the detrusor muscle at equilibrium (B). (n = 10 ± SD, 1 bladder randomised across sampling times).

3.4. Pharmacokinetic modelling

Using STELLA®, a pharmacokinetic model was created to simulate IDD (Figure 7). The model combines differential equations derived from basic pharmacokinetic theory with constants derived from experimentally calculated values (such as the drug's K_p and muscle/blood partition coefficient) to provide a dynamic overview of the factors affecting IDD. Simulations used Euler's method of integration with calculations applied every 0.25 seconds. The model was used to approximate for drug clearance from the bladder wall and the dilution effect of urine, processes that are otherwise absent in our static *ex vivo* experiments. Total urine production by the kidneys was assumed to be 1 ml min^{-1}. Although this rate can vary, 1 ml min^{-1} is a well accepted value for adults [27–29]. For full explanations of the equations / constants utilised in the PK model see supplementary data S.3.

Figure 8 was generated by the model and shows the effects of clearance and dilution on the intravesical delivery process. The constant production of urine will dilute the concentration of drug in the bladder lumen (Fig 8A and B), which is the driving force for the passive diffusion of drug into the bladder wall. The model predicts that this gives rise to a 42% decrease in the drug concentration achieved in the bladder wall after 90 minutes (Fig 8C). Vascular clearance continually carries drug from the bladder tissue into the systemic circulation. The model suggests that this will result in a 24% decrease in bladder wall drug concentration after 90 minutes (Fig 8D). The combination of the dilution effect of the urine and the clearance of drug from the bladder wall results in a predicted 58% decrease in the overall drug concentration achieved in the bladder wall at 90 minutes (Fig 8E).

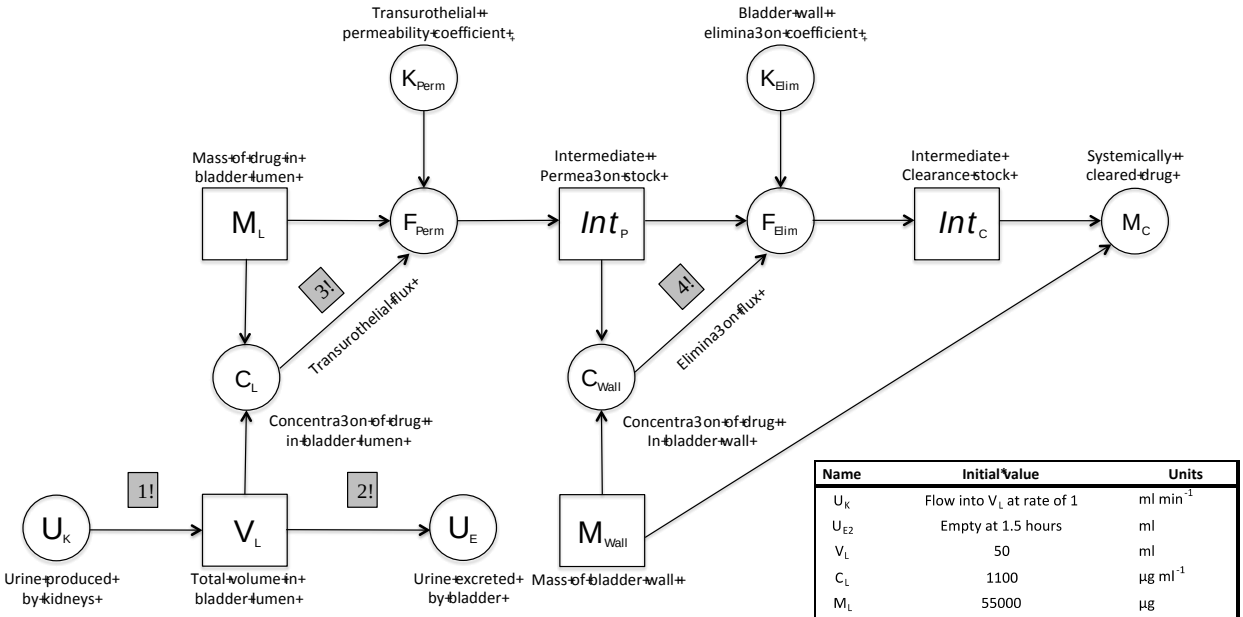

Name	Initial value	Units
U_K	Flow into V_L at rate of 1	ml min^{-1}
U_{E2}	Empty at 1.5 hours	ml
V_L	50	ml
C_L	1100	µg ml^{-1}
M_L	55000	µg
F_{Perm}	$C_L * K_{Perm}$	µg cm^{-2} s^{-1}
K_{Perm}	2.63E-06	cm s^{-1}
C_{Wall}	Int_P * surface area of urothelium exposed /M_{Wall}	µg g^{-1}
M_{Wall}	1	g
F_{Elim}	$K_{Elim} * C_{Wall}$	µg ml^{-1} s^{-1}
K_{Elim}	8.08E-05	s^{-1}
M_{CTotal}	$M_{Wall} * P_U$	µg s^{-1}

!
1:!Dilu(on!of!the!ins(lled!drug!solu(on!by!urine!
2:!Excre(on!of!the!ins(lled!dose!
3:!Transurothelial!permea(on!of!drug!into!the!bladder!wall!
4:!Removal!of!drug!from!the!bladder!wall!into!the!bloodstream!

Fig 7. Overview of the computer-based pharmacokinetic model designed using STELLA®.

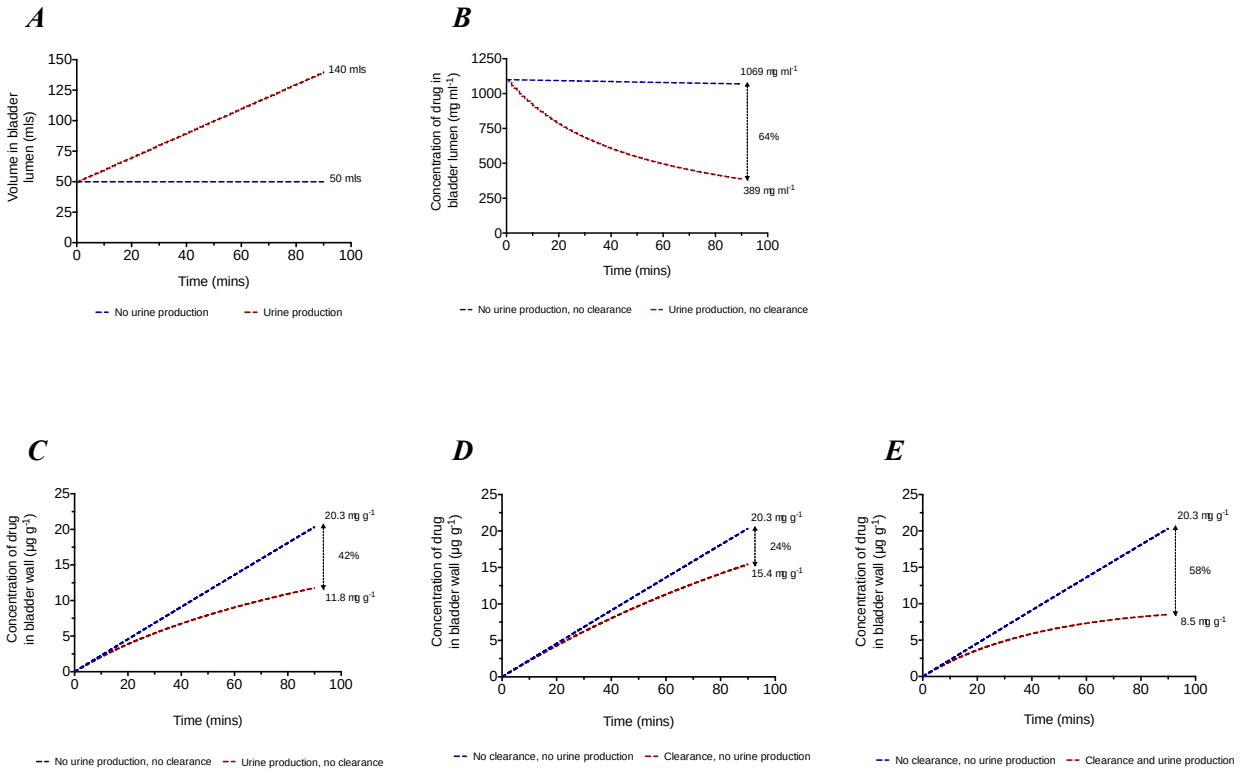

Fig 8. The results of our pharmacokinetic model predictions. For each figure, residual urine = 0 ml, intravesical instillation = 55mg of ketorolac in 50mls saline, K_{Perm} = 2.63 x 10^{-06} cm s^{-1}, K_{Elim} = 8.08 x 10^{-05} s^{-1} (see S.3 for calculation), bladder wall mass = 1g, exposed surface area of urothelium = 1.32 cm^2 and urine production rate = 1 ml min^{-1}. At 90 minutes post intravesical instillation; urine production by the kidneys has increased the bladder volume from 50 to 140 mls (A), resulting in a 64% decrease in the final drug concentration in the bladder lumen (B) (note the luminal drug concentration decreases even in the absence of urine production (1100 to 1069 μg ml^{-1}) due to transurothelial permeation, which is taking place in both scenarios). Subsequently, this results in a 42% decrease in the drug concentration achieved in the bladder wall (C). In the absence of urine production, but including an estimate for vascular clearance, a 24% decrease in the drug concentration achieved in the bladder wall is predicted (D). The combination of urine dilution and clearance gives rise to a 58% decrease in the bladder wall drug concentration (E).

4. Discussion

The aim of this study was to investigate the transurothelial delivery and bladder wall distribution of the NSAID ketorolac using an *ex vivo* porcine model.

Porcine bladder tissue was a natural choice for our *ex vivo* experiments owing to the long history of pigs being used as animal models in urology. A number of studies have reported the physiology of the urinary tract of pigs to be similar to that of humans [30–32].

It was important to ensure that the urothelium remained viable throughout the course of our experiments. A viable barrier would be expected to not only prevent significant permeation, but also differentiate between the transcellular and paracellular movement of molecules. The integrity of the urothelium was evaluated over 6.5 h using two established markers of permeation. Sodium fluorescein was employed as a paracellular marker whilst propranolol hydrochloride was used to represent permeation via the transcellular route. Over 6.5 h the permeation rate of both molecules was constant, indicative of little change in the tissue's behaviour. Furthermore the calculated K_p values (Figure 2A) were distinct and, although there are no directly comparable figures available in the literature, in the same range as those reported for other molecules permeating the urothelium [33].

TEER is an established method of investigating the paracellular permeability of the urothelium [34–37]. By assessing the resistance across bladder mucosa we can evaluate the maintenance of the tight junctions between umbrella cells crucial to the barrier function of the urothelium. Porcine bladder mucosa exposed to saline (control) or ketorolac showed no significant difference in TEER reduction at any timepoint (2.1 and supplementary data S.1). The marginal decrease in TEER with time for all samples was within range of what can be expected for *ex vivo*

experiments such as this. In agreement with our observations, it has recently been shown using TEER that excised, *ex vivo* bladder tissue loaded in side-by-side diffusion cells retains transurothelial barrier function for at least 6 hours [37].

In addition to alterations in tight junction permeability, an increase in paracellular permeability may result from epithelial cell loss [34]. Using SEM we microscopically examined the superficial surface of the *ex vivo* porcine bladder tissue to elucidate urothelial integrity (2.2.3). After 90 minutes the application of saline or ketorolac to bladder tissue loaded in the Franz-cell setup had no significant effect on the morphology of the urothelium (Fig 3 and supplementary data S.2). Scallop-shaped, superficial umbrella cells with intact tight junctions were evident and closely resembled that reported by others [38–40]. Protamine sulfate in a concentration of 10 mg ml^{-1} has been shown to cause immediate umbrella cell sloughing accompanied by a significant decrease in TEER across the urothelium [38]. For this reason protamine sulfate was used as negative control. The urothelium of bladder tissue exposed to protamine sulfate showed a significant loss of integrity with widespread umbrella cell lysis and subsequent exposure of the underlying intermediate cells (Fig 3C and supplementary data S.2).

In combination, the results of investigations into paracellular permeation, TEER and SEM analysis suggest that the *ex vivo* porcine bladder tissue was appropriate for use in our studies.

Recently, Beiko *et al* [41] evaluated the safety and effectiveness of localised, intravesical ketorolac (1.1 mg ml^{-1}) to reduce ureteral stent-related pain. They found a significant reduction in stent-related pain 1 h after stent placement when compared to the control group. While this latest development provides an opportunity for advancing in the management of stent-related pain, its translation into effective patient management will undoubtedly benefit from an understanding of the rate and extent of delivery of ketorolac into the bladder wall. By gathering

information regarding the barrier properties of the urothelium and investigating, in quantitative terms, ketorolac delivery, we can begin to make predictions about the viability of delivering ketorolac intravesically and the bladder tissue concentrations necessary to bring about a therapeutic effect. We chose therefore to use a 1.1 mg ml^{-1} ketorolac solution in our *ex vivo* studies. According to the mean urination time reported, ketorolac would have been voided from the bladder after approximately 90 min explaining our use of this endpoint.

Although the exact aetiology of stent-related pain is unclear, a common theory is that the distal curl of the ureteral stent irritates the urothelium resulting in spasm, aperistalsis and pain [42]. Prostaglandins have been shown to produce contractions of isolated detrusor muscle *in vitro* [43] and their synthesis can be initiated by detrusor muscle stretch and bladder urothelial damage [44]. Blocking prostaglandin synthesis with indomethacin, a non-selective cyclooxygenase (COX) inhibitor, has recently been shown to decrease acetylcholine-mediated autonomic contractions in the isolated bladder [45]. In addition, afferent C-fibres terminating in the urothelium and lamina propria are known to respond to prostaglandins released (from cells in the urothelium and lamina propria) in response to injury [46]; suggesting the possibility that, by inhibiting mediators released from urothelial and lamina propria cells, intravesically delivered NSAIDs (such as ketorolac) may provide pain relief in part via modulation of sensory pathways.

The NSAID ketorolac nonselectively inhibits cyclooxygenase 1 and 2 (COX-1 and COX-2), the enzymes responsible for the production of prostaglandins and has been shown to inhibit ureteral contractility *in vitro* [47]. It follows that by reducing inflammation and spasm, ketorolac should be beneficial in reducing stent-related pain thus explaining its choice by *Beiko et al* [41].

Our permeation study (Figure 4A) shows that ketorolac is capable of permeating across the urothelium (K_p value = 2.63×10^{-6} cm s^{-1}). The production of prostaglandins within the bladder

wall is well established with synthesis occurring not only in the detrusor muscle but also from within the urothelium and lamina propria [43,48–50], both of these regions can therefore be taken to be targets for the IDD of ketorolac. In agreement with others who have performed concentration-depth studies on ex vivo porcine bladder, our distribution study (Figure 5) shows a linear decrease in drug concentration over the urothelium, followed by an exponential decrease in concentration over the lamina propria and detrusor muscle [12,14]. After 90 min the total concentration in these target regions was 87 μg g^{-1}.

To address the absence of dilution by urine and vascular drug clearance from the bladder wall in our experiments, a PK bladder model was built using STELLA®. By visualising complex differential equations, STELLA® enables users to build dynamic models of highly complex systems. The models can be used to investigate the contribution of different variables on the system as a whole. STELLA® is therefore suited to pharmacokinetic (PK) modelling and has been used to develop a range of models including PK profiles for enteric tablets [51], the enhanced oral bioavailability of lipid formulations [52] and ocular permeation following the topical application of drugs [53,54].

Only two intravesical PK models have previously been reported for investigating the effect of physiological and pharmacological parameters upon drug concentrations achieved in the bladder wall [55,56]. The most well known of these was developed in the early nineties by Wientjes et al who used computer-based PK simulations to suggest the optimum dosing strategy for the intravesical delivery of mitomycin C [55]. In contrast to these previous approaches, the user-friendly model described in this study delivers a high resolution PK prediction based on the simultaneous solution of multiple interconnected differential equations. In addition, the speed and flexibility of STELLA® allows the user to rapidly generate a range of PK simulations by

varying determinants such as the rate of urine production, residual urine volume or transurothelial permeation rate. STELLA's® graphical capabilities allow simulations be explored in real time allowing a better and faster understanding of the dynamic processes underlying the intravesical drug delivery process. This capability will be valuable clinicians wishing to explore intravesical dosing regimens for different drugs in the future. We are the first group to demonstrate this kind of real-time, intravesical PK simulations. A muscle/saline partition coefficient was determined to provide an estimate for the *in vivo* muscle/blood partition coefficient for ketorolac. Using this, in conjunction with the calculated K_p value, the PK model was designed to incorporate both the predicted effects of drug clearance and dilution by urine into our permeation data. Vascular clearance and dilution by urine have independent effects on the concentrations of drug achieved in the bladder wall (Fig 8). Importantly the dilution effect was shown to be the more significant of the two, resulting in a predicted 42% decrease in bladder wall drug concentration at 90 minutes (Fig 8C). Our pharmacokinetic model suggests that, due to dilution and vascular clearance, *in vivo* drug concentrations may be 58 % lower than the tissue concentrations determined in the *ex* vivo studies (Figure 5E). Applying this correction factor to the results from the *ex vivo* distribution study (Figure 5) predicts a 90 minute bladder wall drug concentration of 37 $\mu g\ g^{-1}$.

The reported potency of ketorolac, in terms of IC_{50} values, varies widely with top end values of 31.5 and 60.5 μM for COX-1 and COX-2 respectively [26]. Taking the clearance/dilution corrected value of 37 $\mu g\ g^{-1}$ and making the assumption that 1 g of bladder tissue has a volume of ~ 1 cm^3, a ketorolac tissue concentration of 98.3 μM would be achieved 90 minutes after application of 1.1 mg ml^{-1} drug solution. This equates to a ketorolac concentration of at least three times the IC_{50} for COX-1 and one and a half times the IC_{50} for COX-2 at the site of action,

suggesting that levels of ketorolac in the bladder wall would be pharmacodynamically appropriate to provide an anti-inflammatory effect.

In conclusion, using an *ex vivo* porcine approach we have studied the transurothelial permeation of ketorolac and quantitatively investigated its delivery into the different layers of the bladder wall. Using ketorolac as an example, we have shown how fundamental studies such as these can be used to predict the viability of delivering drugs intravesically *in vivo*. It would appear that the levels of ketorolac delivered to the bladder wall following IDD are pharmacodynamically appropriate to provide an anti-inflammatory effect. In practice intravesical dosing is largely guided by clinical outcome, with little information available on target drug concentrations. Investigations such as those described here yield quantitative *ex vivo* data and predictive *in vivo* information that can be used to rationally design new transurothelial drug delivery strategies and optimise existing intravesical drug regimens.

ACKNOWLEDGMENTS

We would like to thank Chris Von Ruhland for his excellent technical assistance. Funding from Boston scientific and the Cardiff School of Pharmacy and Pharmaceutical Sciences is gratefully acknowledged.

SUPPORTING INFORMATION AVAILABLE

Supplementary data (TEER, additional SEM micrographs and explanations of the equations utilised in the STELLA® PK model) is provided. This information is available free of charge via the Internet at http://pubs.acs.org/.

REFERENCES

(1) GuhaSarkar, S.; Banerjee, R. Intravesical Drug Delivery: Challenges, Current Status, Opportunities and Novel Strategies. *J Control Release.* **2010**, *148*, 147–159.

(2) Tyagi, P.; Tyagi, S.; Kaufman, J.; Huang, L.; de Miguel, F. Local Drug Delivery to Bladder Using Technology Innovations. *Urol Clin N Am.* **2006**, *33*, 519–530.

(3) Lewis, S. A.; Diamond, J. M. Na+ Transport by Rabbit Urinary Bladder, a Tight Epithelium. *J Membrane Biol* **1976**, *28*, 1–40.

(4) Lewis, S. A. Everything You Wanted to Know about the Bladder Epithelium but Were Afraid to Ask. *Am J Physiol Renal Physiol* **2000**, *278*, F867.

(5) Williams, T.; Smith, B. *Operating Department Practice A-Z*; 2nd ed.; Cambridge University Press: Cambridge, 2008.

(6) Krambeck, A. E.; Walsh, R. S.; Denstedt, J. D.; Preminger, G. M.; Li, J.; Evans, J. C.; Lingeman, J. E. A Novel Drug Eluting Ureteral Stent: A Prospective, Randomized, Multicenter Clinical Trial to Evaluate the Safety and Effectiveness of a Ketorolac Loaded Ureteral Stent. *J Urol.* **2010**, *183*, 1037–1043.

(7) Mendez-Probst, C. E.; Goneau, L. W.; MacDonald, K. W.; Nott, L.; Seney, S.; Elwood, C. N.; Lange, D.; Chew, B. H.; Denstedt, J. D.; Cadieux, P. A. The Use of Triclosan Eluting Stents Effectively Reduces Ureteral Stent Symptoms: A Prospective Randomized Trial. *BJU Int.* **2012**, *110*, 749–754.

(8) Wientjes, M. G.; Dalton, J. T.; Badalament, R. A.; Drago, J. R.; Au, J. L. S. Bladder Wall Penetration of Intravesical Mitomycin C in Dogs. *Cancer research* **1991**, *51*, 4347.

(9) Wientjes, M. G.; Badalament, R. A.; Wang, R. C.; Hassan, F.; Au, J. L. . Penetration of Mitomycin C in Human Bladder. *Cancer research* **1993**, *53*, 3314.

(10) Wientjes, M. G.; Badalament, R. A.; Au, J. L. . Penetration of Intravesical Doxorubicin in Human Bladders. *Cancer chemotherapy and pharmacology* **1996**, *37*, 539–546.

(11) Kerec, M.; Švigelj, V.; Bogataj, M.; Mrhar, A. The Enhancement of Pipemidic Acid Permeation into the Pig Urinary Bladder Wall. *International Journal of Pharmaceutics* **2002**, *240*, 33–36.

(12) Kerec, M.; Bogataj, M.; Veranic, P.; Mrhar, A. Permeability of Pig Urinary Bladder Wall: The Effect of Chitosan and the Role of Calcium. *Eur J Pharm Sci* **2005**, *25*, 113–121.

(13) Chen, D.; Song, D.; Wientjes, M. G.; Au, J. L.-S. Effect of Dimethyl Sulfoxide on Bladder Tissue Penetration of Intravesical Paclitaxel. *Clin. Cancer Res.* **2003**, *9*, 363–369.

(14) Tsallas, A.; Jackson, J.; Burt, H. The Uptake of Paclitaxel and Docetaxel into Ex Vivo Porcine Bladder Tissue from Polymeric Micelle Formulations. *Cancer Chemother. Pharmacol.* **2011**, *68*, 431–444.

(15) Mugabe, C.; Hadaschik, B. A.; Kainthan, R. K.; Brooks, D. E.; So, A. I.; Gleave, M. E.; Burt, H. M. Paclitaxel Incorporated in Hydrophobically Derivatized Hyperbranched Polyglycerols for Intravesical Bladder Cancer Therapy. *BJU Int.* **2009**, *103*, 978–986.

(16) Mugabe, C.; Raven, P. A.; Fazli, L.; Baker, J. H. E.; Jackson, J. K.; Liggins, R. T.; So, A. I.; Gleave, M. E.; Minchinton, A. I.; Brooks, D. E.; Burt, H. M. Tissue Uptake of Docetaxel Loaded Hydrophobically Derivatized Hyperbranched Polyglycerols and Their Effects on the Morphology of the Bladder Urothelium. *Biomaterials* **2012**, *33*, 692–703.

(17) Mugabe, C.; Matsui, Y.; So, A. I.; Gleave, M. E.; Heller, M.; Zeisser-Labouèbe, M.; Heller, L.; Chafeeva, I.; Brooks, D. E.; Burt, H. M. In Vitro and in Vivo Evaluation of

Intravesical Docetaxel Loaded Hydrophobically Derivatized Hyperbranched Polyglycerols in an Orthotopic Model of Bladder Cancer. *Biomacromolecules* **2011**, *12*, 949–960.
(18) Mugabe, C.; Matsui, Y.; So, A. I.; Gleave, M. E.; Baker, J. H. E.; Minchinton, A. I.; Manisali, I.; Liggins, R.; Brooks, D. E.; Burt, H. M. In Vivo Evaluation of Mucoadhesive Nanoparticulate Docetaxel for Intravesical Treatment of Non-Muscle-Invasive Bladder Cancer. *Clin. Cancer Res.* **2011**, *17*, 2788–2798.
(19) iSEESYSTEMS. Frequently asked questions about STELLA http://www.iseesystems.com/community/support/FAQs.aspx#0 (accessed Oct 25, 2013).
(20) Ro, J. Y.; Ayala, A. G.; el-Naggar, A. Muscularis Mucosa of Urinary Bladder. Importance for Staging and Treatment. *Am J Surg Pathol.* **1987**, *11*, 668–673.
(21) Miodoński, A. J.; Litwin, J. A. Microvascular Architecture of the Human Urinary Bladder Wall: A Corrosion Casting Study. *Anat Rec.* **1999**, *254*, 375–381.
(22) Shen, Z.; Shen, T.; Wientjes, M. G.; O'Donnell, M. A.; Au, J. L. . Intravesical Treatments of Bladder Cancer: Review. *Pharm Res.* **2008**, *25*, 1500–1510.
(23) Hermanns, M. I.; Unger, R. E.; Kehe, K.; Peters, K.; Kirkpatrick, C. J. Lung Epithelial Cell Lines in Coculture with Human Pulmonary Microvascular Endothelial Cells: Development of an Alveolo-Capillary Barrier in Vitro. *Lab Invest.* **2004**, *84*, 736–752.
(24) Walgren, R. A.; Walle, U. K.; Walle, T. Transport of Quercetin and Its Glucosides across Human Intestinal Epithelial Caco-2 Cells. *Biochem Pharmacol.* **1998**, *55*, 1721–1727.
(25) Fromter, E.; Diamond, J. Route of Passive Ion Permeation in Epithelia. *Nature* **1972**, *235*, 9–13.
(26) Laneuville, O.; Breuer, D. K.; Dewitt, D. L.; Hla, T.; Funk, C. D.; Smith, W. L. Differential Inhibition of Human Prostaglandin Endoperoxide H Synthases-1 and -2 by Nonsteroidal Anti-Inflammatory Drugs. *J. Pharmacol. Exp. Ther.* **1994**, *271*, 927–934.
(27) Helms, J. R. Urinalysis and Renal Clearance. In *Mathematics for Medical and Clinical Laboratory Professionals*; Cengage Learning, 2008; pp. 193–202.
(28) Thangarajah, H.; Ghole, S. Quick Reference 2: Renal Facts and Formulas. In *Practical guide to the care of the surgical patient the pocket scalpel*; Mosby/Elsevier: Philadelphia, PA, 2009; p. 18.
(29) Hankins, J.; Intravenous Nurses Society. *Intravenous Therapy: Clinical Principles and Practice*; Saunders: Philadelphia, 1995.
(30) Crowe, R.; Burnstock, G. A Histochemical and Immunohistochemical Study of the Autonomic Innervation of the Lower Urinary Tract of the Female Pig. Is the Pig a Good Model for the Human Bladder and Urethra? *J Urol.* **1989**, *141*, 414–422.
(31) Bridgewater, M.; MacNeil, H.; Brading, A. Regulation of Tone in Pig Urethral Smooth Muscle. *J Urol.* **1993**, *150*, 223–228.
(32) Sibley, G. An Experimental Model of Detrusor Instability in the Obstructed Pig. *Br J Urol.* **1985**, *57*, 292–298.
(33) Sugasi, S.; Lesbros, Y.; Bisson, I.; Zhang, Y. Y.; Kucera, P.; Frey, P. In Vitro Engineering of Human Stratified Urothelium: Analysis of Its Morphology and Function. *J Urol.* **2000**, *164*, 951–957.
(34) Lewis, S. A.; Berg, J. R.; Kleine, T. J. Modulation of Epithelial Permeability by Extracellular Macromolecules. *Physiol. Rev.* **1995**, *75*, 561–589.
(35) Negrete, H. O.; Lavelle, J. P.; Berg, J.; Lewis, S. A.; Zeidel, M. L. Permeability Properties of the Intact Mammalian Bladder Epithelium. *American Journal of Physiology-Renal Physiology* **1996**, *271*, F886.

(36) Janssen, D. A. W.; van Wijk, X. M. R.; Jansen, K. C. F. J.; van Kuppevelt, T. H.; Heesakkers, J. P. F. A.; Schalken, J. A. The Distribution and Function of Chondroitin Sulfate and Other Sulfated Glycosaminoglycans in the Human Bladder and Their Contribution to the Protective Bladder Barrier. *J. Urol.* **2013**, *189*, 336–342.
(37) Erman, A.; Kerec Kos, M.; Zakelj, S.; Resnik, N.; Romih, R.; Veranič, P. Correlative Study of Functional and Structural Regeneration of Urothelium after Chitosan-Induced Injury. *Histochem. Cell Biol.* **2013**.
(38) Lavelle, J.; Meyers, S.; Ramage, R.; Bastacky, S.; Doty, D.; Apodaca, G.; Zeidel, M. L. Bladder Permeability Barrier: Recovery from Selective Injury of Surface Epithelial Cells. *American Journal of Physiology - Renal Physiology* **2002**, *283*, F242–F253.
(39) Lavelle, J. P.; Meyers, S. A.; Ruiz, W. G.; Buffington, C. A. T.; Zeidel, M. L.; Apodaca, G. Urothelial Pathophysiological Changes in Feline Interstitial Cystitis: A Human Model. *American Journal of Physiology - Renal Physiology* **2000**, *278*, F540–F553.
(40) Sun, T.-T. Altered Phenotype of Cultured Urothelial and Other Stratified Epithelial Cells: Implications for Wound Healing. *American Journal of Physiology - Renal Physiology* **2006**, *291*, F9–F21.
(41) Beiko, D.; Watterson, J.; Knudsen, B.; others. A Double-Blinded Prospective Randomized Controlled Trial Assessing the Safety and Efficacy of Intravesical Agents for Ureteral Stent Symptoms Following Extracorporeal Shockwave Lithotripsy. *J Endourol* **2004**, *18*, 723–730.
(42) El-Nahas, A. R.; El-Assmy, A. M.; Shoma, A. M.; Eraky, I.; El-Kenawy, M. R.; El-Kappany, H. A. Self-Retaining Ureteral Stents: Analysis of Factors Responsible for Patients' Discomfort. *J Endourol.* **2006**, *20*, 33–37.
(43) Bultitude, M. I.; Hills, N. H.; Shuttleworth, K. E. Clinical and Experimental Studies on the Action of Prostaglandins and Their Synthesis Inhibitors on Detrusor Muscle in Vitro and in Vivo. *Br J Urol* **1976**, *48*, 631–637.
(44) Rahnama'i, M. S.; van Koeveringe, G. A.; Essers, P. B.; de Wachter, S. G. G.; de Vente, J.; van Kerrebroeck, P. E.; Gillespie, J. I. Prostaglandin Receptor EP1 and EP2 Site in Guinea Pig Bladder Urothelium and Lamina Propria. *J Urol.* **2010**, *183*, 1241–1247.
(45) Rahnama'i, M. S.; van Koeveringe, G. A.; van Kerrebroeck, P. E. V.; de Wachter, S. G. G. The Effect of Indomethacin on the Muscarinic Induced Contractions in the Isolated Normal Guinea Pig Urinary Bladder. *BMC Urol* **2013**, *13*, 8.
(46) Birder, L. A. Nervous Network for Lower Urinary Tract Function. *Int. J. Urol.* **2013**, *20*, 4–12.
(47) Wen, C. C.; Coyle, T. L. C.; Jerde, T. J.; Nakada, S. Y. Ketorolac Effectively Inhibits Ureteral Contractility in Vitro. *J Endourol.* **2008**, *22*, 739–742.
(48) Abrams, P. H.; Sykes, J. A.; Rose, A. J.; Rogers, A. F. The Synthesis and Release of Prostaglandins by Human Urinary Bladder Muscle in Vitro. *Invest Urol* **1979**, *16*, 346–348.
(49) Kasakov, L. N.; Vlaskovska, M. V. Profile of Prostaglandins Generated in the Detrusor Muscle of Rat Urinary Bladder: Effects of Adenosine Triphosphate and Adenosine. *Eur J Pharmacol.* **1985**, *113*, 431–436.
(50) Jeremy, J. Y.; Mikhailidis, D. P.; Dandona, P. The Rat Urinary Bladder Produces Prostacyclin as Well as Other Prostaglandins. *Prostaglandins Leukot Med.* **1984**, *16*, 235–248.

(51) Kambayashi, A.; Blume, H.; Dressman, J. Understanding the in Vivo Performance of Enteric Coated Tablets Using an in Vitro-in Silico-in Vivo Approach: Case Example Diclofenac. *Eur J Pharm Biopharm* **2013**.
(52) Fei, Y.; Kostewicz, E. S.; Sheu, M.-T.; Dressman, J. B. Analysis of the Enhanced Oral Bioavailability of Fenofibrate Lipid Formulations in Fasted Humans Using an in Vitro-in Silico-in Vivo Approach. *Eur J Pharm Biopharm* **2013**.
(53) Ranta, V.-P.; Laavola, M.; Toropainen, E.; Vellonen, K.-S.; Talvitie, A.; Urtti, A. Ocular Pharmacokinetic Modeling Using Corneal Absorption and Desorption Rates from in Vitro Permeation Experiments with Cultured Corneal Epithelial Cells. *Pharm. Res.* **2003**, *20*, 1409–1416.
(54) Grass, G. M.; Lee, V. H. A Model to Predict Aqueous Humor and Plasma Pharmacokinetics of Ocularly Applied Drugs. *Invest. Ophthalmol. Vis. Sci.* **1993**, *34*, 2251–2259.
(55) Wientjes, M. G.; Badalament, R. A.; Au, J. L. Use of Pharmacologic Data and Computer Simulations to Design an Efficacy Trial of Intravesical Mitomycin C Therapy for Superficial Bladder Cancer. *Cancer Chemother. Pharmacol.* **1993**, *32*, 255–262.
(56) Grabnar, I.; Bogataj, M.; Belic, A.; Logar, V.; Karba, R.; Mrhar, A. Kinetic Model of Drug Distribution in the Urinary Bladder Wall Following Intravesical Instillation. *Int J Pharm* **2006**, *322*, 52–59.